WALL THICKNESS - SOLIDIFICATION FEATURES CORRELATION OF DUCTILE IRON CASTINGS UNDER MOULD TYPE INFLUENCE

Irina Varvara ANTON[1], Cristina MILITARU[2], Eduard Marius ŞTEFAN[3], Nicoleta IVAN[4], Mihai CHIŞAMERA[5], Iulian RIPOŞAN[6]

S-au realizat cercetări asupra parametrilor curbelor de răcire şi microstructurii la solidificarea fontei cu grafit nodular sub influenţa tipului formei şi a grosimii de perete. Pentru cercetările experimentale s-au ales trei tipuri de forme (răşină furanică, silicat de sodiu şi bentonită) şi cinci grosimi de perete (8, 14, 22, 31 şi respectiv 40mm). Parametrii curbelor de răcire (CR) ai fiecărei grosimi de perete au fost înregistraţi simultan cu ajutorul unui montaj specific care lucrează în sistemul Labview.

Rezultatele experimentale prezintă corelaţii interesante între parametrii curbelor de răcire şi microstructura probelor turnate sub influenţa tipului formei şi a grosimii de perete.

Some investigations on cooling curve parameters and microstructure of Ductile Iron solidification under mould type and wall thickness influence were made. Three types of moulds (furan resin, Na Silicate and clay-bentonite as binders) and five wall thickness (8, 14, 22, 31 and 40 mm respectively) have been chosen for experimental research. Cooling curves (CC) parameters of each wall thickness were simultaneously recorded by a specific device working in Labview system.

The experimental results give some interesting corelations between cooling curves parameters and cast samples microstructure under mould type and wall thickness influence.

Keywords: Ductile iron, solidification, mould type, wall thickness, cooling curves parameters, microstructure

[1] PhD student, Faculty of Materials Science and Engineering, University POLITEHNICA of Bucharest, Romania, e-mail: aniv2k1@yahoo.com
[2] PhD student, Faculty of Materials Science and Engineering, University POLITEHNICA of Bucharest, Romania
[3] PhD student, Faculty of Materials Science and Engineering, University POLITEHNICA of Bucharest, Romania
[4] PhD student, Faculty of Materials Science and Engineering, University POLITEHNICA of Bucharest, Romania
[5] Prof.. Faculty of Materials Science And Engineering, University POLITEHNICA of Bucharest, Romania
[6] Prof., Faculty of Materials Science And Engineering, University POLITEHNICA of Bucharest, Romania

1. Introduction

Ductile Iron (DI) microstructure is strongly influenced by the dynamics of the thermal equilibrium involved in the mould during casting solidification and its solid state cooling. The thermal equilibrium character is determined by iron melt pouring temperature, pouring rate, thermophysical properties of the mould, cast piece wall thickness etc. Thermal analysis is one of the most common techniques used to relieve the correlation between the thermal equilibrium modifications and microstructure evolution during primary or secondary transformations. The thermal analysis includes a high unexploited potential for more investigations to clarify the mechanism of iron melt solidification and structure and mechanical/technological properties prediction. In this respect many investigations are focused generally speaking on cast iron solidification, but a special attention is accorded to DI solidification [1-6].

2. Experimental procedure

The paper objective is to establish some correlations inbetween the solidification conditions (mould type, wall thickness), cooling curves (CC) parameters and DI microstructure (graphite, matrix).

In this respect, three sand mould types (bentonite, sodium silicate and furan resin respectively) were used and three step wedge test samples (see the pattern designed in fig.1) were poured from an eutectic D.I.

The main thermophysical properties of the three mould types are presented in table 1 while, the charge materials and the nodulizer/inoculant chemical compositions are presented in table 2 and table 3 respectively. As seen in table 1 the sodium silicate base sand mould has the highest cooling capacity while the bentonite base (dry mould) and the furan resin mould have a similar lower cooling capacity.

The step wedge test block has five different wall thickness steps as: 8 mm, 14 mm, 22 mm, 31 mm and 40 mm respectively (the dimensions are that resulted after cast samples solidification).

For cooling curves recording K type thermocouples were assembled into the mould, one for each sample's step and a Labview soft based device was used both for data recording and their processing (including the first and the second derivatives).

Table 1

Thermophysical properties of mould sands

Nr. crt.	Mould materials	b_f modulus, $W \cdot s^{1/2}/m^2 \cdot grd$	Density ρ, kg/m^3	Specific heat, c_p, J/kg·K	Conductivity, λ, W/m·K
1.	Bentonite base sand (dry mould):	1368	1650	1090	1.04

	15% betonite 5% water 85% silica sand				
2.	Na Silicate base sand: 10% sodium silicate 90% silica sand	1865	1700	1312	1.56
3.	Furan resin base sand: 3% furan resin 1.5% intensifier 95.5% silica silica sand	1306	1550	1170	0.94

The base iron was prepared in an acid line induction furnace (80kg capacity, 2400 Hz frequency) using a normal charge recipe: 50%high purity pig iron, 40% ductile iron scrap and 10% steel scrap (see table 2). The nodulizing treatment was realized by Tundish-Cover technique using FeSiCaMgRE as a nodulizer alloy (2.0% rate addition) while the inoculation by ladle treatment technique with Foundry Grade (FG-FeSi) inoculant (0.5% rate addition) – see tabel 3.

The thermal regime of iron melt processing consisted of 1550^{o}C superheating temperature, 1530^{o}C taping (nodulizing) temperature and 1350^{o}C pouring temperature.

Table.2

Chemical composition of charge materials

Charge materials	C %	Mn %	Si %	P %	S %	Other elements %
High purity pigiron (50%)	3.95	0	0.088	0.013	0.004	Cr – 0.008; Mo – 0.005 Ni – 0.072; Al – 0.002 Cu – 0.02; Ti – 0.003 V – 0.16; W – 0.004
Ductile Iron scrap (40%)	3.64	0.47	2.55	0.02	0.016	Cr – 0.04; As – 0.005; V – 0.001; Ti – 0.002
Steel scarp (10%)	0.22	0.50	0.28	0.055	0.055	-

Table.3

Chemical composition of FeSiCaMgRE nodulizer and Ca-FeSi inoculant

Alloy \ Chemical Composition %	C	Si	Al	Ca	Mg	RE
FeSiCaMgRE (Nodulizer)	-	46.7	0.76	1.06	9.21	0.95
FG-FeSi (Inoculant)	0.04	73	1.25	0.3	-	-

For chemical composition investigation the OES coin samples were taken by SAF-DO400 foundry sampler device.

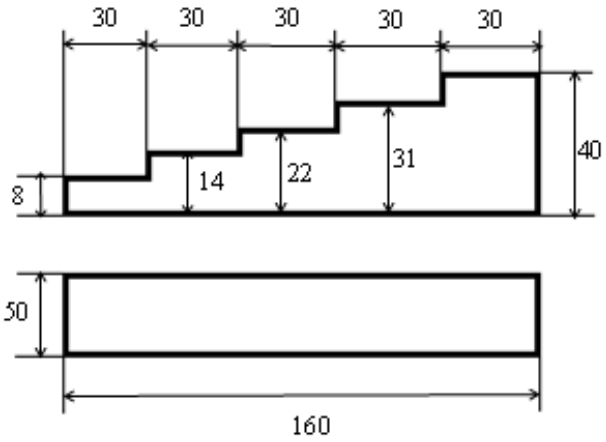

Fig.1. Schematic representation of wedge test block pattern

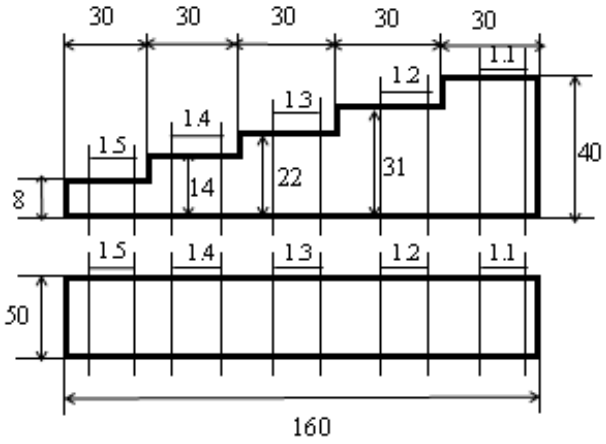

Fig.2. Schematic representation of samples taken out from the test block

The samples cut from step wedge test block (fig.2) have been polished for metallographic examination to reveal the graphite morphology and the matrix structure analysis. In this respect an automat image analysis system was used.

A general schematic representation of cooling curve for eutectic Ductile Iron is showen in fig.3.

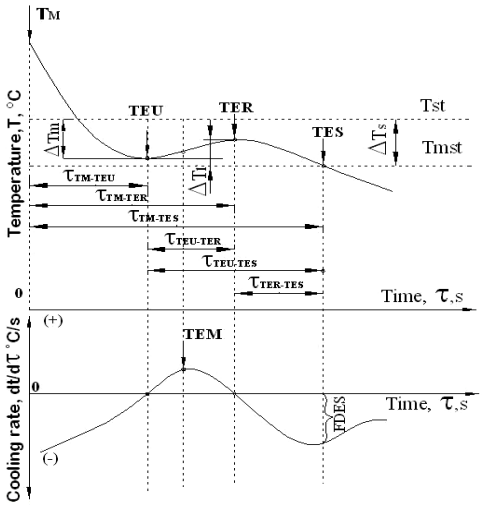

TM - maximum temperature of the poured melt,^{o}C;
TEU - temperature of eutectic undercooling,^{o}C;
TER - temperature of the graphitic recalescence,^{o}C;
TES - temperature of the end of solidification (end of solidus)^{o}C;
TEM - maximum recalescence rate, ^{o}C/sec;
Tst – graphitic eutectic equilibrium temperature,^{o}C;
Tmst – carbide eutectic equilibrium temperature,^{o}C;
ΔTm – maximum degree of undercooling (ΔTm = Tst-TEU),^{o}C;
ΔTr – recalecence degree (ΔTr = TER-TEU),^{o}C;
$\tau_{TM-TEU}...\tau_{TER-TES}$ – the durations of different stages (or cumulated stages) along sample cooling/solidification.
FDES - minimum value of the first derivative of cooling curve at the end of eutectic solidification, ^{o}C.

Fig.3. Cooling curves pattern of eutectic Ductile Iron solidification:

3. Results

3.1. Chemical composition

The chemical composition both for base untreated and final DI are presented in table 4.

Table 4

Chemical composition of the obtained Ductile Iron

Cast Iron	Ad. %	Chemical composition, %						Elements, %	CE %
		C	Si	Mn	P	S	Mg		
Base cast iron	-	3.84	1.22	0.510	0.0162	0.0132	0.00042	Cr-0.0317%;Al-0.0010%; Cu-0.0325%;Ti -0.0039%; Pb-0.0018;Sn-0.0025 %; As-0.0036%;Ca<0.00020%; Sb-0.00040%;La<0.00010%; N-0.0104%; Fe-94.5%	4.06
Final DI	• 2.0% FeSiCa MgRE • 0.5% FGFeSi	3.52	2.52	0.507	0.0169	0.012	0.0445	Cr-0.0346%;Al-0.0165%;Cu-0.0348%;Ti-0.0063%;Pb-0.0048;Sn-0.0035%;As-0.0037%;Ca> 0.0060%;Sb-0.00071%;La-0.0050%;N-0.0084%;Fe-93.4%	4.27

3.2. Cooling curves analysis

The general aspect of the fourtheen CC (one thermocouple failed) is presented in fig.4 while, the main CC parameters are presented in table 5. Based on CC parameters, the cooling rates (CR) in different stages of iron melt solidification were calculated (tabel 6), using the following relationship:

$$CR = \frac{\Delta T}{\Delta \tau}, \ ^{o}\text{C/s}$$

where: ΔT is the temperature variation in the time range Δτ.

For example:

$$CR_{TM-TEU} = \frac{TM - TEU}{\tau_{TEU} - \tau_{TM}}, \ ^{o}\text{C/s}$$

where: $CR_{TM\text{-}TEU}$ is the cooling rate in TM-TEU temperature range.

One can remark the heating effect in the TEU-TER range, thus will have a heating rate, because of latent solidification heat releasing.

The influence of wall thickness on the main cooling curves parameters as well as, the cooling rate, for the three mould types are presented in fig.5, fig.6 and fig.7 respectively.

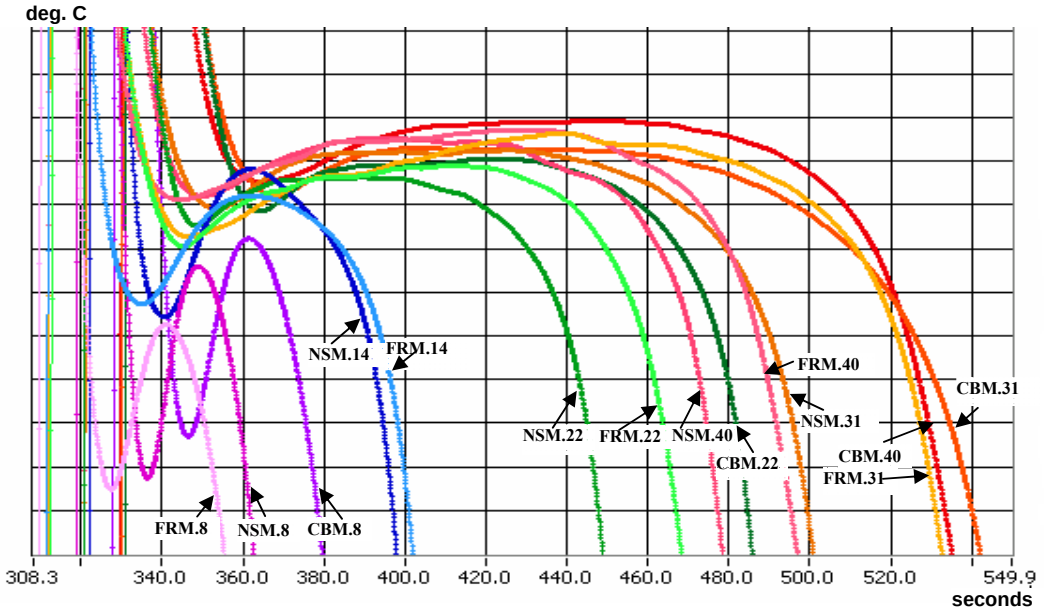

Fig.4. Cooling curves aspect for different mould types and wall thickness:
FRM.8....40 – Furan resin mould (8...40 mm wall thickness)
NSM.8....40 – Sodium silicate mould (8...40 mm wall thickness)
CBM.8....40 – Clasical bentonite (dry) mould (8...40 mm wall thickness)

Table 5

Cooling curves parameters depending on wall thickness and mould type, for different stages of ductile cast iron solidification (see also fig.3)

Mould type	Cooling curves parameters											
	δ, mm	M*, cm	Tst	Tmst	T_M	TEU	TER	TES	TEM	FDES	ΔTm	ΔTr
Furan resin	8	0.33	1169.9	1116.8	1224.8	1133.0	1140.5	1089.6	0.881	-3.41	36.9	7.5
	14	0.50	1169.9	1116.8	1207.8	1141.5	1146.4	1107.7	0.323	-2.66	28.4	4.9
	22	0.69	1169.9	1116.8	1207.8	1144.1	1147.8	1114.4	0.176	-1.75	25.8	3.7
	31	0.82	1169.9	1116.8	1219.6	1144.5	1149.2	1113.5	0.124	-1.82	25.4	4.7
	40	0.86	1169.9	1116.8	1216.6	1146.2	1149.4	1104.7	0.105	-1.40	23.7	3.2
Sodium silicate	8	0.33	1169.9	1116.8	1226.8	1133.5	1143.2	1084.2	1.30	-4.46	36.4	9.7
	14	0.50	1169.9	1116.8	1202.2	1140.9	1147.6	1103.3	0.563	-3.40	29.0	6.7
	22	0.69	1169.9	1116.8	1212.7	1145.0	1147.3	1116.1	0.166	-2.60	24.9	2.3
	31	0.82	1169.9	1116.8	1210.1	1145.8	1148.5	1106.5	0.153	-2.28	24.1	2.7
	40	0.86	1169.9	1116.8	1205.7	1146.4	1149.1	1106.0	0.114	-2.13	23.5	2.7
Bentonite	8	0.33	1169.9	1116.8	1221.1	1136.4	1144.5	1088.9	1.01	-3.77	34.5	9.1
	22	0.69	1169.9	1116.8	1209.7	1145.7	1148.1	1117.6	0.159	-2.30	24.2	2.4
	31	0.82	1169.9	1116.8	1215.2	1146.4	1148.5	1109.9	0.12	-1.49	23.5	2.1
	40	0.86	1169.9	1116.8	1218.4	1147.1	1149.8	1112.4	0.105	-1.33	22.8	2.7

* - the coresponding cooling modulus of the sample steps.

Table 6

Cooling rate - wall thickness - mould type dependence in different stages of ductile cast iron solidification (see also fig.3)

Mould type	δ, mm	M*, cm	Cooling rate (°C/sec) in the ranges:					
			TM-TEU	TM-TER	TM-TES	TEU-TER**	TEU-TES	TER-TES
Furan resin	8	0.33	6.12	2.96	2.34	0.56	1.02	1.74
	14	0.50	3.24	1.31	1.05	0.19	0.46	0.80
	22	0.69	2.14	0.63	0.58	0.06	0.23	0.52
	31	0.82	2.39	0.48	0.47	0.04	0.16	0.43
	40	0.86	2.36	0.56	0.56	0.04	0.25	0.56
Sodium silicate	8	0.33	6.44	3.10	2.67	0.78	1.26	2.22
	14	0.50	3.91	1.48	1.21	0.32	0.57	0.99
	22	0.69	2.72	0.88	0.74	0.04	0.27	0.55
	31	0.82	2.17	0.61	0.55	0.04	0.24	0.48
	40	0.86	2.24	0.62	0.63	0.04	0.32	0.64
Bentonite	8	0.33	5.50	2.51	2.12	0.61	1.00	1.76
	22	0.69	2.12	0.68	0.58	0.04	0.22	0.45
	31	0.82	2.00	0.63	0.47	0.03	0.19	0.33
	40	0.86	2.23	0.58	0.49	0.03	0.19	0.39

* - the coresponding cooling modulus of the sample steps.

** - heating rate

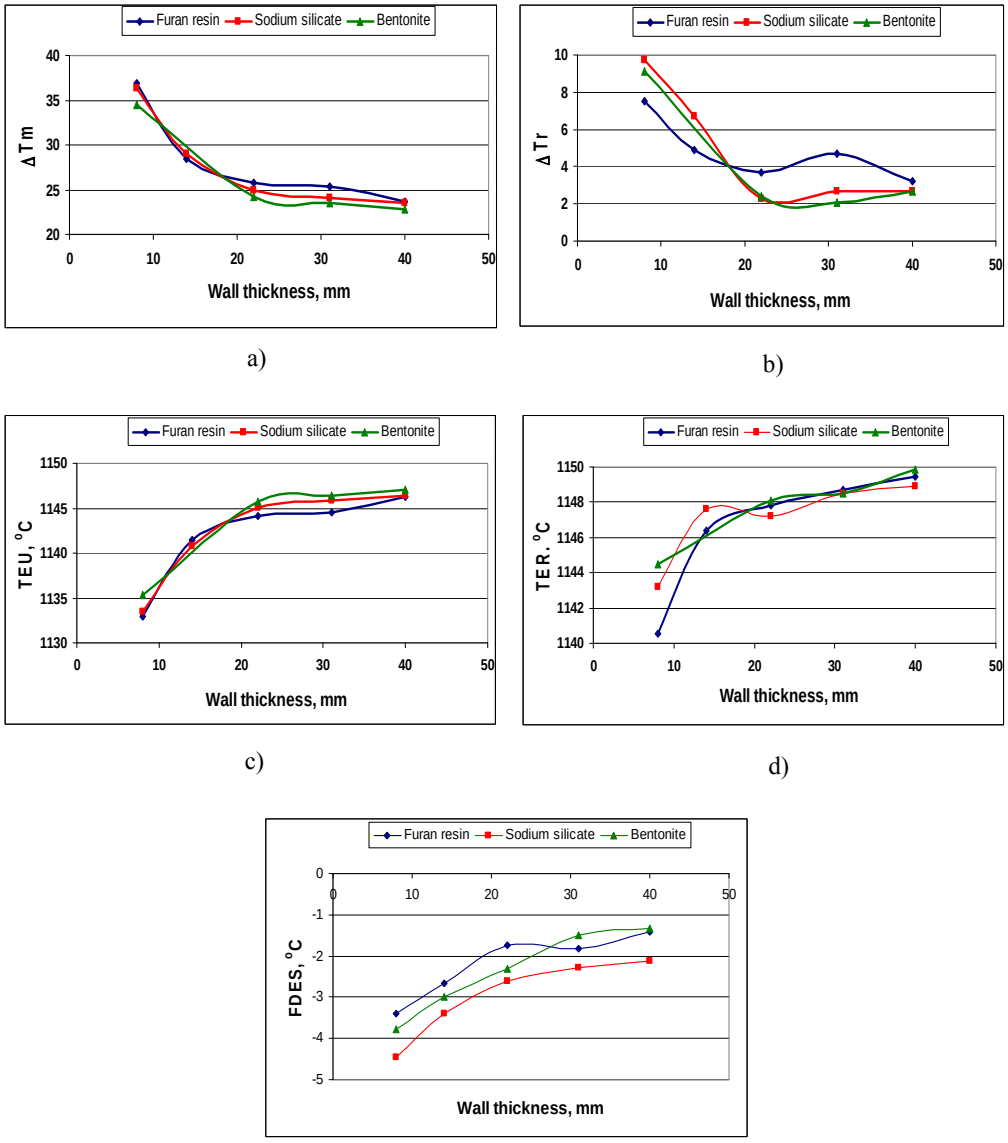

Fig. 5. Cooling curves parameters depending on wall thickness, under mould type influence (see also Fig.3. and table 5)

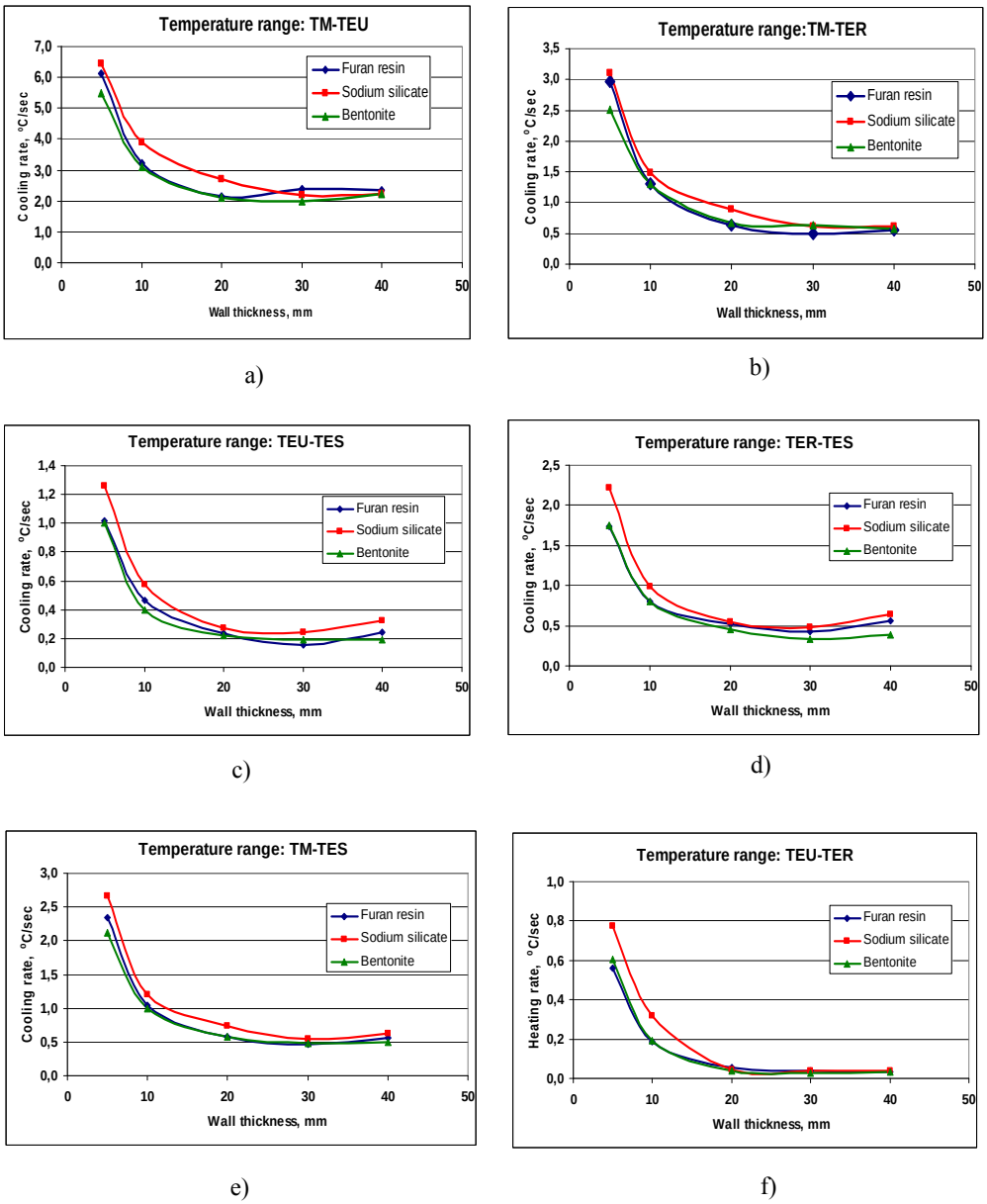

Fig. 6. Cooling rate-wall thickness dependence for different stages of DI solidification:
a) TM-TEU; b) TM-TER; c) TEU-TES; d) TER-TES; e) TM-TES; f) TEU-TER (heating rate)

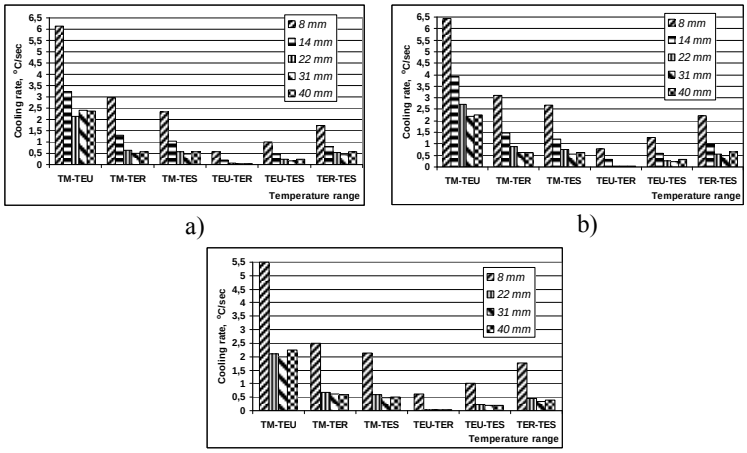

Fig. 7. Cooling rate evolution in different stages of step wedge test block sample solidification: a – furan resin mould; b – sodium silicate mould; c – bentonite mould;

3.3. Structure analysis

The main features of DI microstructure for the five steps and the three mould types are presented in table 7, fig.8 and fig.9 while the aspect of graphite and matrix structure in table 8 and table 9, respectively.

Table7

DI microstructure parameters under wall thickness /mould type influence (five fields average)

Mould type	Wall thickness, mm	Graphite analysis				Matrix, %	
		Surface %	Density N_n, 1/mm^2	Feret mean diameter, µm	Shape factor	Ferrite	Pearlite
Furan resin	8	14.8	466	16.7	0.87	80	20
	14	14.6	459	16.9	0.85	85	15
	22	14.6	437	16.9	0.86	80	20
	31	15.0	426	17.2	0.85	85	15
	40	15.6	414	17.3	0.86	85	15
Sodium silicate	8	14.9	484	14.6	0.87	60	40
	14	15.2	471	14.8	0.87	65	35
	22	15.3	458	15.3	0.86	70	30
	31	15.5	442	15.1	0.85	70	30
	40	15.5	436	16.0	0.85	85	25
Bentonit	8	14.6	473	15.8	0.87	70	30
	14	14.6	465	16.3	0.86	75	25
	22	14.8	441	16.6	0.87	80	20
	31	15.3	435	17.1	0.86	85	15
	40	15.4	427	17.1	0.85	85	15

- **Density Nn,1/mm^2** – nodules count - spot surface ratio; **Feret mean diameter, µm** – the mean distance of parallel tangents at opposing particle borders; **Shape factor** – it provides information about the „roundness“ of the particle. For a spherical particle the shape factor is 1, for all other particles it is smaller than 1.

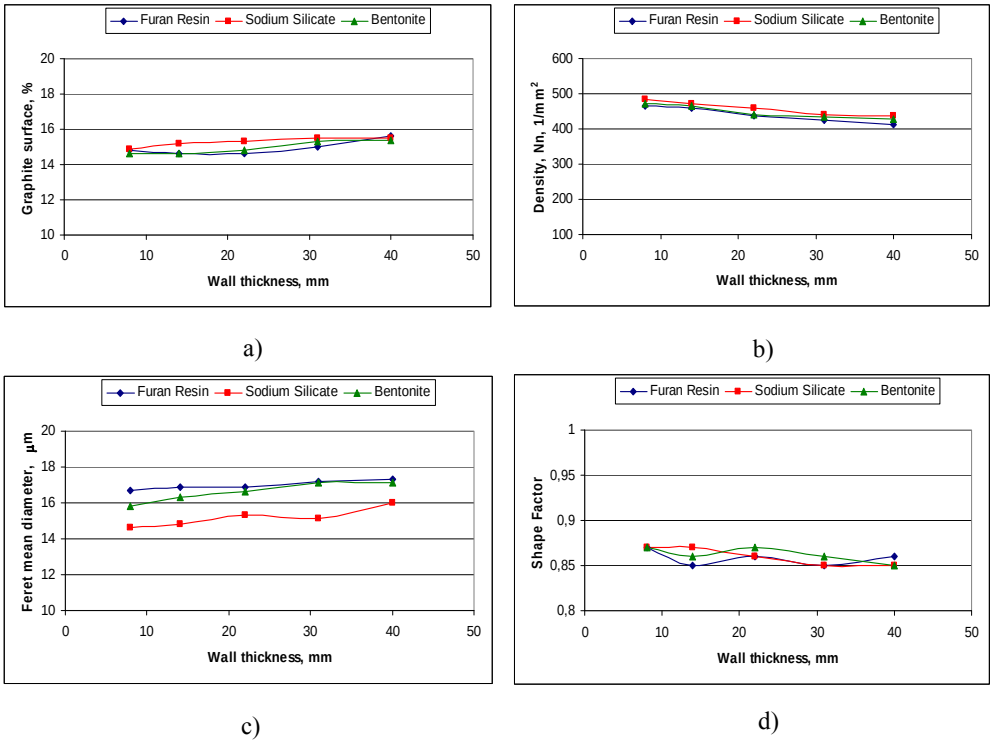

Fig. 8. Graphite structure parameters – wall thickness dependence under mould type influence

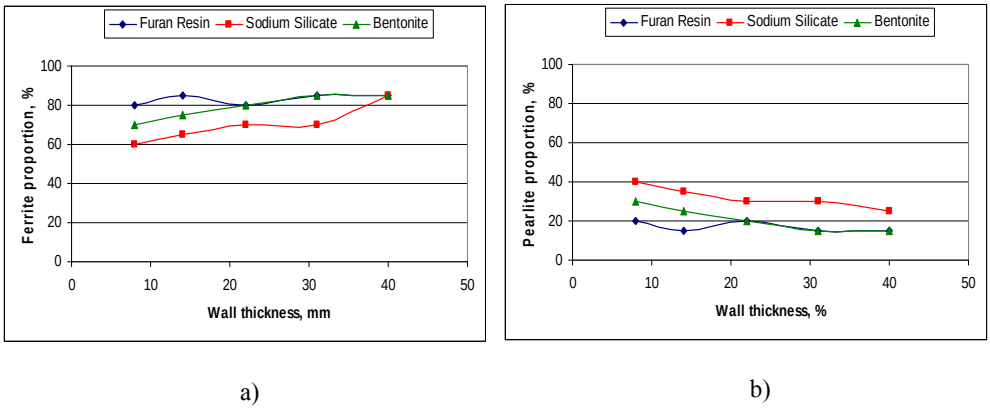

Fig. 9. Ferrite/pearlite ratio under wall thickness/mould type influence

Table 8

Influence of wall thickness/mould type on graphite morphology

$\frac{\delta, mm}{(M/cm)}$	Furan Resin mould	Na Silicate mould	Bentonite mould
$\frac{8}{0.33}$	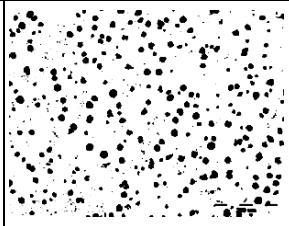	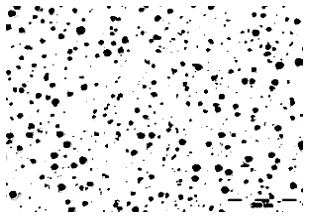	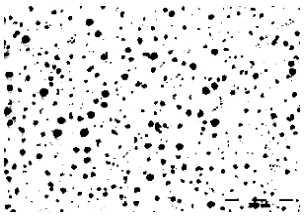
$\frac{14}{0.50}$	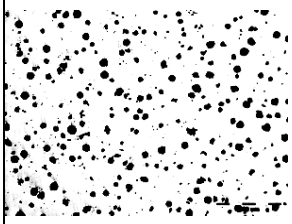	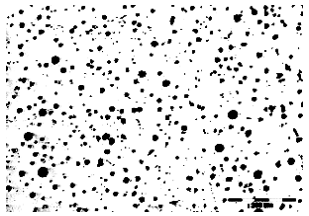	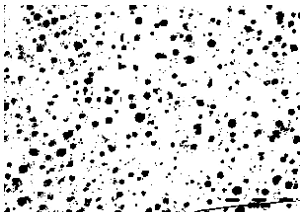
$\frac{22}{0.69}$	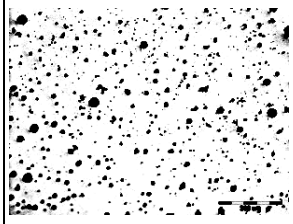	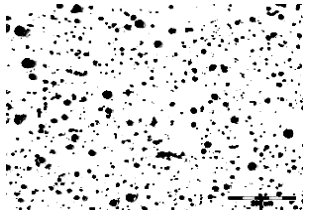	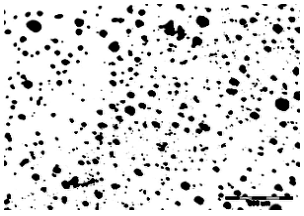
$\frac{31}{0.82}$	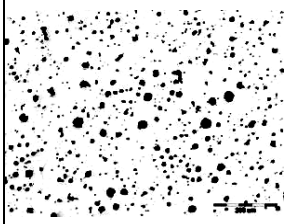	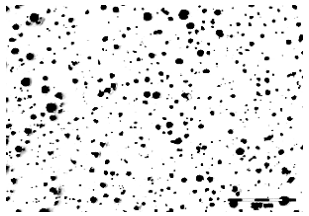	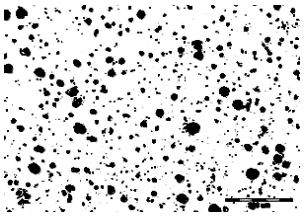
$\frac{40}{0.86}$	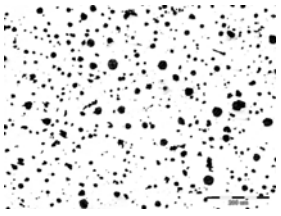	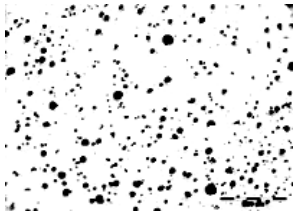	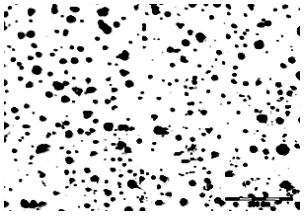

Table 9

Influence of wall thickness/wall type on the matrix structure

$\frac{\delta, mm}{(M/cm)}$	Furan Resin mould	Na Silicate mould	Bentonite mould
$\frac{8}{0.33}$	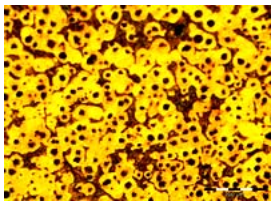	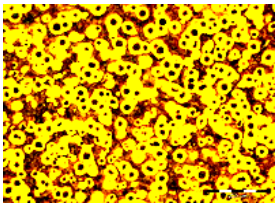	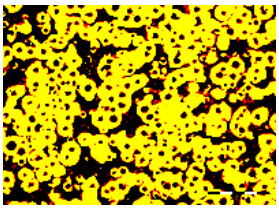
$\frac{14}{0.50}$	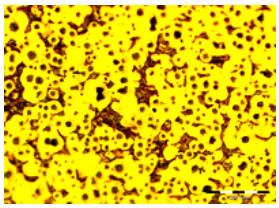	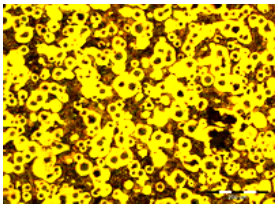	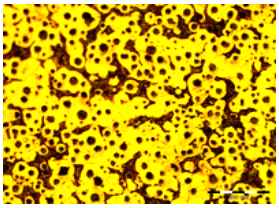
$\frac{22}{0.69}$	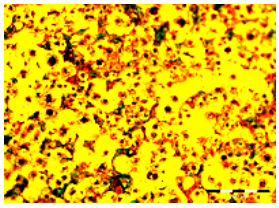	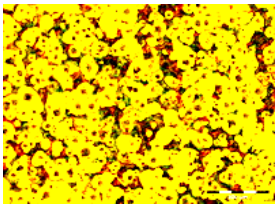	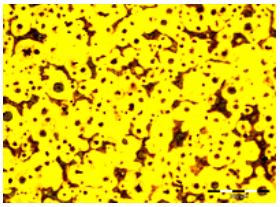
$\frac{31}{0.82}$	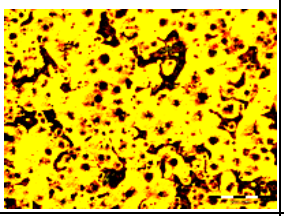	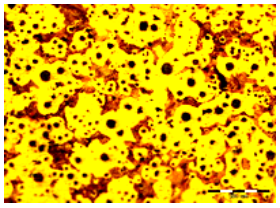	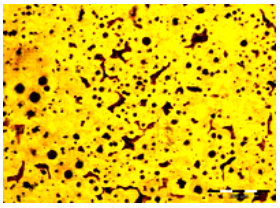
$\frac{40}{0.86}$	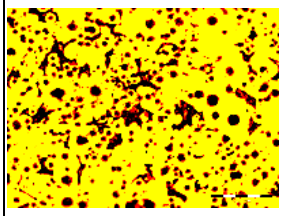	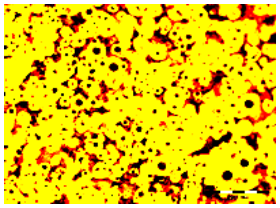	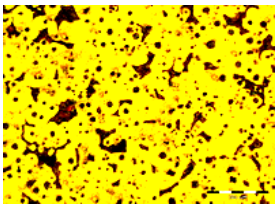

4. Discussion

Both wall thickness and mould type influence on DI behaviour on solidification were investigated using a normal eutectic composition (CE = 4.27%) – see table 4.

The cooling curves aspects were strongly affected especially by wall thickness but in a much lower degree by mould type (table 5, fig.5).

Both eutectic undercooling (ΔTm) and eutectic recalescence (ΔTr) clearly decrease with wall thickness increasing (fig.5. a, b) while minimum (TEU) and maximum (TER) eutectic temperature increase (fig.5. c, d) which is quite normal.If the three moulds are compared from this point of view, no clear differences could be noted. However, the cooling rate-wall thickness dependence graphs (fig.6) show a much clearer difference of the three moulds each other for all solidification stages (fig.6). As one can see, the cooling rate is higher in case of Na silicate base mould and similarly but on lower level in case of furan resin and bentonite moulds. The differences between the three types of moulds are bigger on smaller wall thickness and they become smaller on higher wall thickness (table 6, fig.6). This fact may be put in connection with the heat absorbtion/transmission capacity of the moulds which decreases as the heat amount increases (the cast wall thickness increases). In all cases the cooling rate – wall thickness dependence has an exponential decreasing variation on small sizes. As fig.7 shows, for all samples steps the highest cooling rate was recorded in TM – TEU temperature range while the lowest (heating effect) in TEU – TER range that is, when the eutectic crystalization becomes intensive (first stage of eutectic graphitization).

In all cases the cooling rate increases in the final stage of eutectic graphitization because of decreasing of liquid ratio (the heat extraction by the mould becomes dominant given the solidification latent heat releasing). If the wall thickness is considered, as from fig.7 results, there is a big difference inbetween the 8 and 14 mm sizes on one hand and 22, 31 and 40 sizes on the other hand as cooling rate (the cooling rate is more equilibrated at the higher sizes for all types of mould and all solidification stages). This could suggest on the liquid metall migration from the largest size to the smallest one which determines a heat balance equalization inbetween the three sections and a slight increase of the cooling rate in the largest section. The head effect contributes to the decrease of the cooling rate difference between these sections.

If the first derivative value (FDES) on the end of solidification (TES) is considered (see table 5, Fig.5 c) a smaller shrinkage tendency is expected to be obtained in case of Na Silicate mould in comparison with the other two mould types (the higher negative value of FDES the lower shrinkage tendency of cast

iron). This is because of the higher rigidity of the Na Silicate mould as compared to the other two moulds.

The structure analysis also shows a better dependence by wall thickness than mould type for this kind of moulds which can be considered as a confirmation of cooling curves parameters variation. So, from fig.8 and table 7 one can see a clear dependence of graphite parameters, especially nodules count, nodules size and graphite ratio by wall thickness and a realtive less influence of sample size on the graphite shape factor (fig.8 d) for these ranges of wall size variation. By comparing the mould types each other some clearer effect seems to be exerted by the Na Silicate mould which determines some finer graphite structure given the other two mould types which have a close influence.

As the results from table 8 and fig. 9 show, the matrix structure is clear influenced in a higher degree by wall thickness than mould type. Wall thickness increasing gives a higher ferrite ratio despite of some coarser graphite structure.If mould types are compared, a slight difference can be noted inbetween them (a higher pearlite ratio on Na Silicate mould and close similar level of pearlite ratio on furan resin and bentonite mould). Both graphite and matrix structure changing under wall thickness and mould type influence are in good agreement with cooling curves parameters and thermal analysis,so using all these techniques one can obtain a more detailed information about the mechanism of DI structure formation.

5. Conclusions

Some investigations were caried out concerning the DI solidifications under wall thickness (8...40mm) and mould type (Furan Resin, Na Silicate and Bentonite base sand mould respectively) influence.

The main ideas resulting from this experiment could be summarized as follows:

- Both wall thickness and mould type have a clear influence an DI solidification but for the analyzed moulds the wall thickness influence is stronger.
- Na silicate base sand mould gives somewhat higher cooling rate along the all solidification range in comparison with the bentonite and the furan resin moulds which have a close behaviour. This is because the higher thermal conductivity of the former and the closer but at a lower level of thermal conductivity of the last two moulds.
- The cooling rate is changing along the solidification range being higher in the TM-TEU range and lowest in the TEU-TER range when a heating effect is recorded. This is because of the thermal balance created by latent heat of solidification.

- In the last part of eutectic solidification the cooling rate increases for all sample sizes and mould types because of decreasing of the latent heat contribution to the thermal balance.
- A smaller shrinkage tendency is expected to be obtained in case of Na Silicate mould in comparison with FRM and dry CBM because of the higher negative level of the first derivative value (FDES) at the end of solidification of the former.
- DI structure (graphite and matrix) is in good corelation with the cooling curves parameters variation under wall thickness and mould type influence.
- The more detailed investigations are intended in the future to clarify other aspects of DI solidification such as iron melt-mould interaction and graphite degeneration in the cast skin both under wall thickness and mould type influence.

R E F E R E N C E S

[1] *M. Chisamera, I. Riposan, S. Stan, P. Toboc, T. Skaland, D. White*, Shrinkage Evaluation in Ductile Iron as Mould / Inoculant Type Influence. In: Proceedings of the SPCI 8 International Symposium on Science and Processing of Cast Iron, Oct. 2006, Beijing, China, Tsinghua University Press, 2006, p. 116-121

[2] *I. Riposan, M. Chisamera, S. Stan, C. Gadarauteanu, T. Skaland,* Analysis of Cooling and Contraction Curves to Identify the Influence of Inoculants on Shrinkage Behavior of Ductile Irons. In: Proceedings of 2003 Keith Millis Symposium on Ductile Cast Iron, Oct. 2003, Hilton Head Island, USA, p. 125-135

[3] *M. Chisamera, S. Stan, I. Riposan, E. Stefan, G. Costache,* Thermal Analysis of Inoculated Grey Cast Iron., UGALMAT, Galati, Oct. 2007, Tehnologii si Materiale Avansate, Galati University Press, **vol. 1**, p. 17-23

[4] *M. Chisamera, I. Riposan, S. Stan, T. Skaland,* Cooling Curves Analysis of the Ca/Sr Overinoculated Grey Irons, at Lower Initial Silicon Content. SoCaS-The Science of Casting and Solidification International Conference, Brasov, Romania, 28-31.05.2001, p. 330-335

[5] *M. Chisamera, I. Riposan, Ed. Stefan, G. Costache,* Thermal analysis control of in-mould and ladle inoculated grey cast iron, China Foundry, **vol. 6**, No 2, May 2009, p. 145-151.

[6] *M. Chisamera, I. Riposan, S. Stan, Chris Ecob, Geir Grasmo, David Wilkinson,* Preconditioning of electrically melted grey cast irons, U.P.B Sci.Bull, Series B, **vol.71**, Iss.3, 2009.